The Knee 54 (2025) 71–80

Contents lists available at ScienceDirect

The Knee

journal homepage: www.elsevier.com/locate/thekne

A deep learning and statistical shape modeling-based method for assessing intercondylar notch volume in anterior cruciate ligament reconstruction ☆

Anna Ghidotti [a,*], Daniele Regazzoni [a], Miri Weiss Cohen [b], Caterina Rizzi [a], Vincenzo Condello [c]

[a] Department of Management, Information and Production Engineering, University of Bergamo, Bergamo, Italy
[b] Department of Software Engineering, Braude College of Engineering, Karmiel, Israel
[c] Joint Conservative and Reconstructive Surgery Unit – Sports Traumatology, Humanitas Castelli Clinics, Bergamo, Italy

ARTICLE INFO

Article history:
Received 18 June 2024
Revised 24 October 2024
Accepted 6 February 2025

Keywords:
Automatic segmentation
Deep learning
Statistical shape modelling
ACL injury
Principal component analysis
Anatomical variation

ABSTRACT

Background: Anterior cruciate ligament (ACL) reconstruction is a widely performed procedure for ACL injury, but there are several factors which may lead to re-rupture or clinical failure. An intercondylar notch (or fossa) that is narrower may increase the likelihood of injury. Traditional two-dimensional assessments are limited, and three-dimensional (3D) volume analysis may offer more detailed insights. This study employs deep learning and statistical shape modeling (SSM) to enhance 3D modeling of the intercondylar notch, aiming to gain a deeper understanding of this complex 3D anatomical region.
Methods: A methodology was developed to generate accurate 3D models of the intercondylar fossa within seconds. The variability of the intercondylar notch in ACL-injured samples was analyzed using SSM techniques, focusing on its principal components. Additionally, gender differences in notch volume were examined using *t*-tests.
Results: The best deep learning method for automatic segmentation of the notch was SegResNet, which achieved a Dice similarity coefficient of over 0.88 and a Hausdorff distance of 0.73 mm. The small volume-related relative error (0.06) illustrates the goodness of the result. Three principal components accounted for 72.59% of the variation, including notch volume, shape, width, and height. Females had statistically significant smaller notch compared with males with ACL injury ($P < 0.001$).
Conclusion: By examining notch volume and its variability in ACL-injured patients, it is possible to understand the complex anatomy of the intercondylar notch and tailor ACL reconstructions accordingly.

1. Introduction

The anterior cruciate ligament (ACL) is one of the most frequently injured ligaments of the knee joint, with an incidence rate of 68.6 injuries per 100,000 person-years [1]. ACL reconstruction (ACL-R) is widely recognized as one of the most effective treatment options for individuals who suffer from functional instability due to a torn ACL [2]. Several factors

☆ This article is part of a special issue entitled: 'AI and new technologies' published in The Knee.

* Corresponding author at: Department of Management, Information and Production Engineering, University of Bergamo, Via Pasubio 7b, 24044 Dalmine BG, Italy.
E-mail address: anna.ghidotti@unibg.it (A. Ghidotti).

https://doi.org/10.1016/j.knee.2025.02.009
0968-0160/

may contribute to a re-rupture or clinical failure in an ACL-R patient, including the graft size and location [3]. Small-diameter hamstring autografts (<0.8 cm) tend to re-injure and even marginal increases in their size (0.5-mm increments) can reduce graft rupture rates. However, large grafts may impinge on the femoral notch and adversely affect healing [4]. The risk of impingement with ACL-R and hamstring autografts varies depending on the graft diameter, the placement of the tunnel, and the geometry of the intercondylar notch, within which the graft is housed. A narrow intercondylar notch (or fossa) may impose additional mechanical stress on the graft, increasing the likelihood of injury.

Several two-dimensional (2D) parameters, including notch width, notch width index, notch angle, notch depth, and notch shape index are largely employed for identifying the morphology of the femoral intercondylar notch [5]. Nevertheless, these parameters are usually location- and plane-dependent, and they are not suitable for describing the complex three-dimensional (3D) structure of the intercondylar notch. An analysis of its 3D volume may provide more detailed information that can be utilized in quantitative analysis [6]. Literature concerning notch volume has two major limitations. Firstly, there is a scarcity of literature due to labor-intensive and time-consuming measurements conducted on several slices in order to measure the notch volume. Secondly, the literature is quite diverse, for instance in terms of measurement methods or differential analysis, concerning the gender. Similarly to other 2D notch parameters, notch volume also varies significantly between genders. The notch volumes of women with ACL injuries are smaller and there is little heterogeneity among them. As a result of smaller notches and thinner ACLs, female athletes are more likely to sustain injuries than their male counterparts [5].

Currently, notch volume is being studied as a potential risk factor for ACL rupture, by comparing healthy and diseased individuals [7–9]. It is unclear from literature whether patients elected for ACL-R display anatomical variability in the size and shape of the femoral intercondylar fossa [3,10]. Providing a detailed description of the anatomical variations found in the intercondylar notch will contribute to a better understanding of this complex regional anatomical structure. An analysis of the variability in the intercondylar notch can be useful in planning the size and placement of grafts for each patient. Statistical shape modeling (SSM) techniques can be employed to evaluate the variability in shapes among populations [11]. An examination of the differences between knees with an ACL injury and healthy knees was conducted using these techniques [12–14]. Pedoia et al. [12] found that intercondylar narrowing is the second source of variability between healthy and ACL-injured patients. However, the variability within a group of patients with ACL injuries remains to be determined. The study conducted by Zrojkiewicz et al. [3] examined the variability of the fossa in relation to impingement risk in ACL-injured patients, but they used two-dimensional images in their approach.

This study aims to enhance the intercondylar notch volume assessment in ACL-R with deep learning (DL) and SSM techniques. The objective is to better understand how much notch volume is a source of variability, which needs to be taken into account when performing an ACL reconstruction. To achieve this, a methodology is developed for generating accurate 3D models of the intercondylar fossa. The variability of the intercondylar notch in an ACL-injured sample is analyzed, using SSM techniques. The innovation lies in the description of the relationship among morphological features within each component in 3D.

2. Materials & methods

The proposed approach involves four stages, represented in Figure 1. The first stage involves patient selection. Secondly, variations of U-Net segmentation architectures, which are deep learning (DL) models, including 3D U-Net [15], Attention U-Net [16], SegResNet [17] and VNet [18] were used to automatically segment the intercondylar notch. Thirdly, a morphological analysis of the reconstructed 3D models of the intercondylar notch was performed. An evaluation of the degree of variability was conducted by developing a statistical shape model and examining its principal components (PCs). Finally, statistical analyses were also conducted to investigate gender differences in the volume of the notch.

Figure 1. Workflow of the proposed approach. DL, deep learning; SSM, statistical shape modeling.

2.1. Patient selection

This research was a retrospective morphological study approved by the institutional review board of Humanitas Gavazzeni and Castelli, private hospitals in Bergamo, Italy. Informed consent was obtained from all individual participants included in the study. Medical images of 109 patients who underwent a magnetic resonance (MR) scan of their knee joint for an ACL injury between January 2022 and July 2023 were acquired in two clinical centers using an ad hoc protocol of proton density weighted (PDW) sequence with a slice thickness of 0.55 mm. From the original MR images, seven patients were excluded due to revision surgery and two for image quality issues. Consequently, 100 ACL-injured patients were considered (Figure 2).

Table 1 summarizes the characteristics of the selected patients, including 31 females and 69 males.

2.2. DL for automatic segmentation

DL techniques, in particular 3D convolutional neural networks (CNNs), were used to automatize segmentation process to obtain intercondylar notch. 3D CNNs have become a prominent framework for medical image segmentation due to their ability to effectively process and analyze 3D medical images, such as MR volumes. Hence, 3D U-Net [15], Attention U-Net [16], SegResNet [17] and VNet [18] were employed for their ability to segment medical images.

The U-Net architecture, introduced by Ronneberger et al. [15] is a specialized DL framework designed for segmenting neuronal structures in electron microscopy images. It employs a unique encoder–decoder network configuration, with the encoder extracting high-level features from the input image, and the decoder generating the segmentation mask. U-Net differentiates itself from traditional segmentation methods that rely on manually crafted features by autonomously deriving features from the data [19,20]. The U-Net network consists of interconnected encoders and decoders with skip connections. The encoder network resembles a standard CNN, employing convolutional and pooling layers to decrease spatial resolution while increasing feature maps. Each convolutional layer is followed by a rectified linear unit (ReLU) activation function to introduce nonlinearity. Through training, the encoder network becomes adept at learning high-level features in the input image. The U-Net decoder network employs convolutional and upsampling layers to increment spatial resolution while reducing feature maps. The decoder's primary role is to create the segmentation mask by combining high-level features from the encoder with low-level features from the input image. The inclusion of skip connections between the encoder and decoder allows for the integration of low-level and high-level features by concatenating feature maps from corresponding layers. This integration enhances the network's ability to accurately segment complex and small objects. The attention mechanism in Attention U-Net allows the network to dynamically focus on important parts of the image while ignoring irrelevant areas. This is achieved through attention gates, which filter the features propagated through the network based on their relevance

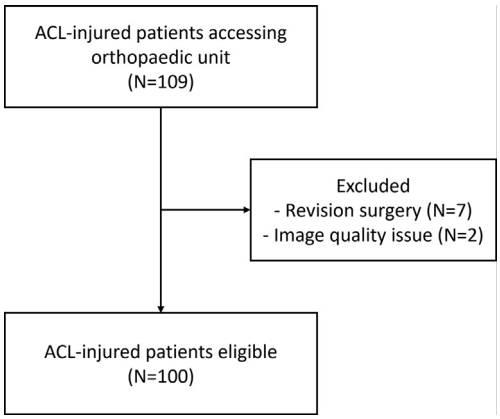

Figure 2. Flow diagram of patient selection. ACL, anterior cruciate ligament.

Table 1
Patient age and height divided by gender.

	Female	Male	P
Sample number	31	69	–
Age, years	31.56 ± 13.75	30.74 ± 11.31	0.765
Height, cm	166.91 ± 5.23	180.09 ± 6.86	<0.001

According to one-way analysis of variance (ANOVA) test, there is no statistically significant difference in age between genders, but there is a statistically significant difference in height between genders.

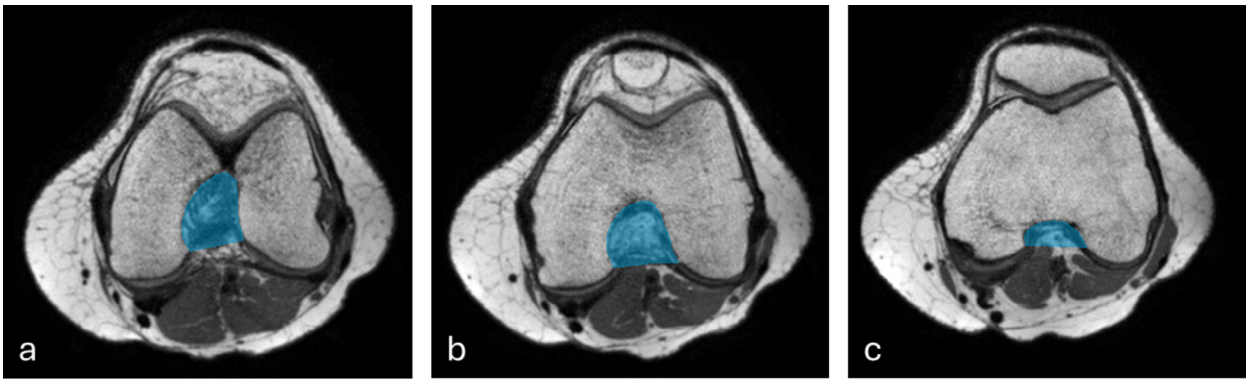

Figure 3. Axial slices of knee magnetic resonance showing the femoral intercondylar notch volume measurement. (a) The slice with continuity between the medial and the lateral femoral condyles; (b) An intermediate slice; (c) The slice with both femoral condyles visible.

[16]. SegResNet uses residual connections from the ResNet architecture. ResNet addresses the vanishing gradient problem by using residual blocks with skip connections. Through these connections, one or more layers are bypassed by adding the input of a block to its output, effectively creating a shortcut. The process increases weight values sufficient to allow simplifying the optimization (backpropagation) process and improving performances [17]. V-Net is a neural network architecture designed for the segmentation of 3D volumetric medical images. To handle volumetric data efficiently and capture spatial context across multiple dimensions, it utilizes 3D convolutions and residual connections. Similar to U-Net, V-Net uses residual connections inspired by ResNet to facilitate its training phase, thus providing the ability to learn residual mappings and allowing it to optimize segmenting 3D volumetric images [18].

The selected CNNs required two inputs. The first input was MR images, that were augmented using data augmentation techniques such as linear transforms and rotation, resulting in 276 volumes of data.

The second input was the labels of the intercondylar notch. They were obtained using van Eck's method [7]. Anatomic landmarks were used to define its boundaries in each slice of the axial MR images [4–6]. First axial slice showing both condyles was considered to be the superior starting point of the intercondylar notch. This finding was confirmed by sagittal views. In the last axial slice with continuity between the medial and lateral femoral condyles with their cartilage clearly visible, the inferior endpoint of the notch was identified. In Figure 3, the first, a middle, and the last axial slices to identify the intercondylar notch are shown.

The augmented MR dataset was randomly divided into 75% for training, 20% for validation and 5% for testing. During the training, hyperparameter optimization was performed to achieve the best results for each net. In particular, two hyperparameters that influence the model's performance and accuracy were chosen. The former is epoch, which is the number of times the entire dataset is passed forward and backward through the neural network during the training process. It is varied between 50 and 100 epochs. The latter is the learning rate, that determines the step size at each iteration during the training process. It controls how quickly the model learns by adjusting the weights of the network in response to the estimated error. It is varied between 10^{-3} and 10^{-5}.

To test the reliability of the trained network models, a test set was used. Dice similarity coefficients (DSCs) and Hausdorff distances (HDs) were considered as evaluation metrics. DSC is a statistical metric commonly used to quantify the degree of similarity or overlap between two sets. The coefficient is a value between 0 and 1, where 0 indicates no overlap, and 1 represents perfect agreement or complete overlap between the sets. The formula for DSC describes the ratio between two times the intersection of the sets over their sum:

$$DSC = \frac{2TP}{2TP + FP + FN} \tag{1}$$

Distance is commonly employed to assess the similarity between the automatic segmented region and the ground truth. HD measures how far the furthest point in a set is from its nearest neighbor in the other set. The formula is as follows

$$HD(A,B) = \max_{a \in A} \left\{ \min_{b \in B} \{d(a,b)\} \right\} \tag{2}$$

where a and b are points of sets A and B respectively and $d(a,b)$ is the distance between a and b.

Moreover, the volume relative error was calculated as the ratio of the absolute difference between automatic and manual segmentation over the manual segmentation of the test set.

$$Volume\ relative\ error = \frac{|Volume_{automatic} - Volume_{manual}|}{Volume_{manual}} \tag{3}$$

For the purpose of the study, an open-source framework for DL in healthcare imaging, Medical Open Network for AI [21], was employed together with MONAI Label, setting in 3D Slicer software [22]. The training of the nets was performed using the following hardware components: Intel(R) Xeon(R) W-2245 CPU @ 3.90 GHz and GPU NVIDIA RTX A5000.

2.3. Anatomical variation using SSM

Based on the segmented intercondylar notches, a statistical shape model was developed to evaluate shape variability among patients with ACL injuries. SSM is a technique used to analyze and represent the geometric variability of shapes within a dataset using statistical methods. It aims to capture the main modes of variation in shapes and quantify these variations in a compact and interpretable form. In the present study, the SSM package of Materialise 3-matic was used to create and analyze the SSM [23].

Initially, the intercondylar notch of the right knee was mirrored to the left for uniformity. Then, a random model was used as a source and uniformly re-meshed. A remeshing process was performed such that each shape was represented by an equal number of L corresponding vertices. Consequently, each shape was represented by a vector with $M = 3 \times L$ dimensions (x, y, z coordinates). Then, the shapes were aligned in space in order to eliminate translation and rotation, according to general Procrustes analysis (GPA). The Procrustes distance is a measure of difference between shapes, and was minimized for all shapes by translating and rotating each shape. After vectorization and alignment phases, Principal component analysis (PCA) was performed to determine the principal modes of shape variation. PCA transforms correlated shape variations into uncorrelated variables known as PCs or mode of variations, and orders them by their magnitude of variability. Collectively, these components characterize the major sources of shape diversity observed in the intercondylar notch dataset.

SSM quality was assessed using two measures. Compactness was the first metric, defined as the number of PCs required to describe a fixed percentage of variation. Generalization was the second metric, which represents how well a random notch can be described using the developed SSM. It is based on computing the average distance between the original notch mesh and the mesh obtained by the SSM [11].

Based on literature [5,24], five relevant parameters were identified and measured, shown in Figure 4. They are notch volume, notch width in coronal (NWc) and axial (NWa) view, notch height (NH) and depth (ND). These parameters were determined on the mean shape of the fossa, and on other 3D models obtained varying from −3 standard deviation (SD) to + 3 SD for the first three modes of variation.

2.4. Gender comparison

In addition, volume parameter was measured on 100 patients to evaluate the difference between male and female. *t*-Test was performed to test for significant differences ($P < 0.001$) in this parameter between gender [25]. Additionally, the correlation between notch volume and height of the patients was calculated in order to determine whether the difference between males and females is dependent on the size of the patients.

3. Results

3.1. Automatic segmentation performance

The performance of the selected DL models was evaluated on the testing dataset in accordance with the defined metrics. Table 2 presents the average results for DSC, HD, and relative error for each CNN. The best DL method was SegResNet, trained for 50 epochs at a learning rate of 10^{-3}, which achieved a DSC of over 0.882 and an average HD of 0.730 mm. In this case, the goodness of the result can be demonstrated by the small relative error related to the volume (0.062).

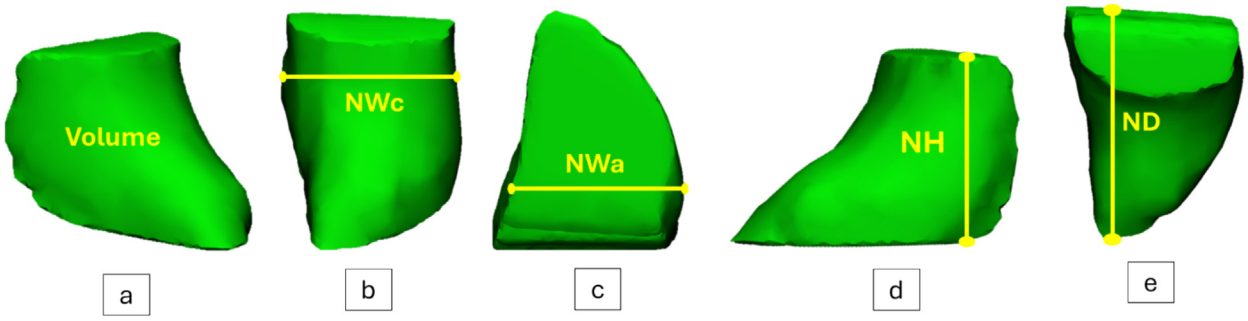

Figure 4. (a) Notch volume; (b) notch width in coronal view (NWc); (c) notch width in axial view (NWa); (d) notch height (NH); (e) notch depth (ND).

Table 2
Dice similarity coefficient (DSC), Hausdorff distance (HD) (mm) and volume relative error of the chosen deep learning (DL) methods.

DL model	DSC	HD (mm)	Volume relative error
UNet	0.877 ± 0.016	0.775 ± 0.105	0.104 ± 0.036
AttentionUNet	0.869 ± 0.023	0.821 ± 0.139	0.095 ± 0.033
SegResNet	**0.882 ± 0.026**	**0.730 ± 0.176**	**0.062 ± 0.055**
VNet	0.868 ± 0.027	0.829 ± 0.189	0.076 ± 0.061

All values are shown as mean ± standard deviation.

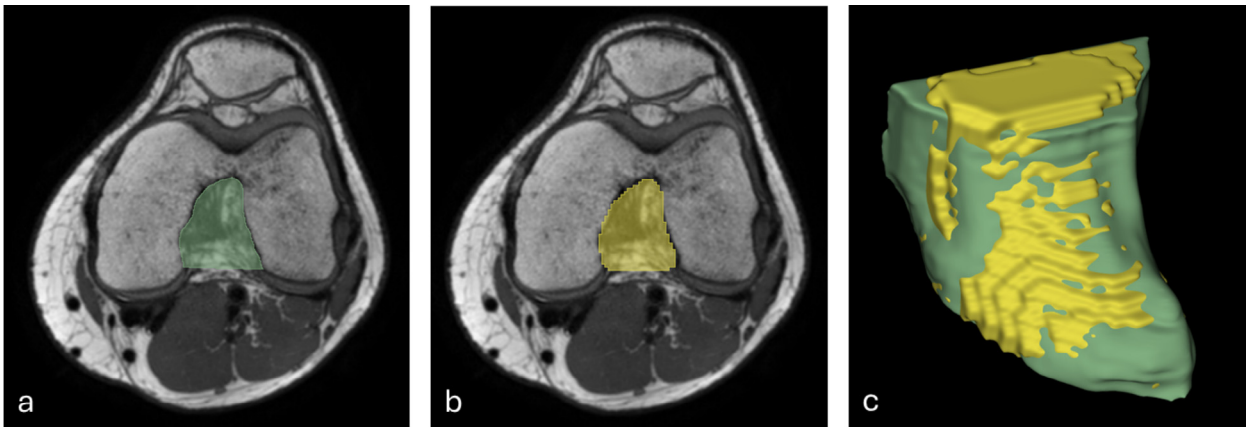

Figure 5. Manual (a) and automatic (b) segmentation in the axial plane. The volumes are overlapped (c) to compute Dice similarity coefficient (DSC), Hausdorff distance (HD) and volume relative error. It is presented the case of a patient with a DSC achieved 0.908, HD is 0.557 and the volume relative error is 0.042.

Figure 5 illustrates the comparison between the sections predicted from manual segmentation of the intercondylar notch (Figure 5(a)) and the automated segmentation (Figure 5(b)) and of the volume (Figure 5(c)), using SegResNet. The intercondylar notch volumes between manual and automatic segmentation showed strong correlation across intercondylar notch, with Pearson's coefficient r value of 0.897.

3.2. Morphological analysis

Three components accounted for 72.59% of the anatomical shape variation of the intercondylar notch. The first PC represented 46.70%, the second contributed 20.37%, the third accounted for 5.52% (Figure 6). Generalization shows that a random notch can be described by the SSM with an average accuracy of 0.690 mm. To visualize the shape characteristics of each PC, the shape that corresponded to extreme values was plotted, as shown in Figure 6.

To quantify shape changes, morphological parameters were measured and reported in Table 3. The first mode of variation is related to the size and the notch volume changes from −57% (−3 SD) to + 92% (+3 SD), as compared with the mean shape. A second PC can be attributed to the notch shape. Looking at the three overlapped shapes (−3 SD, mean, +3 SD) in Figure 7, it is evident a shape change. While for the mean model and + 3 SD model, it is recognized a U-shape, for the −3 SD model, an A-shape is recognized [26]. This second mode of variation is related to the width of the notch, both from the coronal and axial perspectives: it varies from −28% (−3 SD) to + 29% (+3 SD) and from −20% (−3 SD) to + 20% (+3 SD) in the coronal and axial plane, respectively. The third mode of variation showed a variation in the notch height, even if the percentage of variation is less, compared with the previous modes.

Regarding the intercondylar notch volume, the differences between males and females are shown in Figure 8. The notch volumes of males and females with ACL injury were 8.55 ± 1.47 and 6.43 ± 1.51 cm^3, respectively. Females had smaller notch compared with males with ACL injury ($P < 0.001$).

To understand whether this result is related to patient size, the volume of the intercondylar notch was compared with the patient's height. Pearson's coefficient r indicates a moderate correlation ($r = 0.65$).

4. Discussion

The aim of the present study was to enhance the intercondylar notch volume assessment in ACL-R by using DL and SSM techniques. The main finding is that the intercondylar notch volume is the first and main source of variability in ACL-injured patients. Specifically, the volume explains 46.7% of the overall observed variance, followed by notch shape, notch width and notch height.

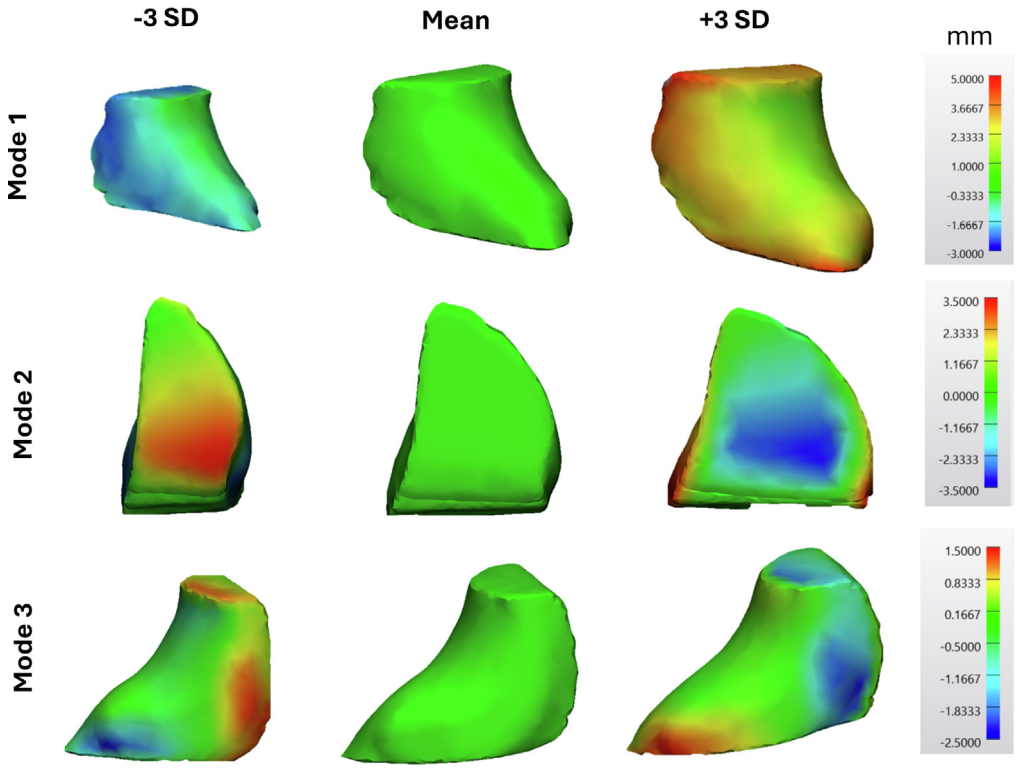

Figure 6. Mean shape of the intercondylar notch of anterior cruciate ligament-injured patients varied by ± 3 standard deviation (SD) along the first three principal components. The colors represent the distance in millimeters from the mean shape.

Table 3
A description of the principal components, expressed as a percentage of variation.

	Mean	Mode 1		Mode 2		Mode 3	
		−3 SD	+3 SD	−3 SD	+3 SD	−3 SD	+3 SD
Volume	7.788 cm^3	**−57%**	**92%**	−2%	−5%	−3%	1%
NW coronal	22.72 mm	−28%	24%	**−28%**	**29%**	5%	−11%
NW axial	19.17 mm	−25%	23%	**−20%**	**20%**	−6%	8%
NH	22.39 mm	−27%	29%	24%	−14%	**11%**	**−10%**
ND	30.37 mm	−21%	26%	11%	0%	−6%	8%

The percentage values in bold indicate the most relevant. ND, notch depth; NH, notch height; NW, notch width.

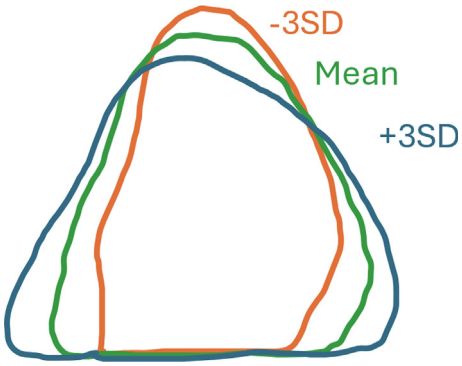

Figure 7. Mode 2 shows an intercondylar notch shape variation. This is confirmed by the notch width measurement. SD, standard deviation.

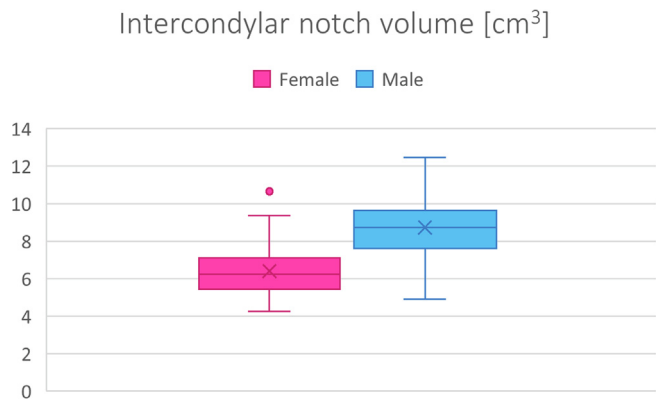

Figure 8. Box plot of the intercondylar notch volume of female and male measured in cm^3.

The use of 3D volumes has only been utilized recently for the evaluation of intercondylar notch size, but, as confirmed in this study, it is well suited for representing the complex 3D structure of the intercondylar notch, overcoming the limitations of 2D parameters. Van Eck et al. [7] were the first to investigate whether intercondylar fossa volume was related to ACL injury. Actually, they measured intercondylar notch volumes of 6.5 cm^3 and 5.9 cm^3 in patients with and without ACL injuries, respectively. Several other studies have examined the 3D volume of the intercondylar notch, finding that patients with ACL injuries have a smaller intercondylar notch compared with the control group [8,9,27]. Intercondylar notch volumes reported in the aforementioned studies of ACL-injured patients were slightly lower than the value of 7.788 cm^3 found in the present study. This discrepancy may be caused by the way in which the volume was obtained. All of the previous researches involved manual tracking of the boundaries of the notch in 2D medical images. The area of each slice is calculated and multiplied by the slice thickness, which is typically 3.0 mm in traditional methods. Compared with the previous investigations, the thickness of the slice in the present study was 0.55 mm, and the volume was automatically computed by the software, multiplying the number of voxels in the segment by the voxel size. As a result of such a small slice thickness, it is possible to obtain extremely accurate 3D volumes, which are ideal for the purposes of this study.

Manually identifying the intercondylar notch on each slice is time consuming, and as a result, its volume assessment is less diffuse than two-dimensional parameters, which are quicker and simpler to compute. To increase accessibility to 3D volumes, a procedure was developed as part of the present study. The proposed method, which uses DL algorithms, provides a 3D volume in only 5–10 s, compared with 10–15 min for manual segmentation. The accuracy of the automatic segmentation achieved was compared with manual labeling, with a DSC value more than 0.88 and HD less than 0.73 mm. This high DSC value indicates a strong agreement between the automated segmentation and manual labeling, underscoring the reliability and precision of the selected DL models. Furthermore, the low volume relative error (0.062) demonstrated the reliability of the selected DL models for the computation of intercondylar notch volume. DL was particularly effective due to its capability to learn complex patterns and features directly from data. As a result of training on a diverse dataset, which encompasses a variety of intercondylar notch shapes, DL models become adept at capturing the inherent variability between patients. Only Li et al. [6] tried to automatize the intercondylar fossa, reaching good accuracy, employing a ResU-Net. A number of studies have utilized DL techniques to automate knee joint segmentation, focusing on the bones, ligaments, muscles, cartilage, tendons, vessels, and nerves, without considering the notch fossa [28–30]. In this regard, there was a need to automate this region, as it contains important information for patients who have sustained an ACL injury. Therefore, the present study examined DL algorithms commonly used in medical image segmentation, including the 3D U-Net, AttentionU-Net, VNet, and SegResNet.

In investigating the anatomical variability of the intercondylar fossa volume, gender influences were taken into consideration. The intercondylar notch volume showed significant differences for sex comparison in the set of 100 patients. Similar results were found by Fayad et al. [31] in 63 knees. Wolters et al. [32] stated that women had a smaller notch and a smaller insertion site than men. The same conclusion was reached by Jha et al. [5], who assessed the difference in notch volume between the ACL-injured and uninjured in men and women combined or stratified by sex. The small notch volume may be one of the reasons for females being more likely to suffer an ACL injury than males. It is reported that tears of the ACL are two to eight times more common in females than males [31]. Besides having smaller knees than men due to their smaller skeletons, there are a number of other possible causes, both internal and external [6]. In this study, there is a moderate correlation between intercondylar notch volume and the patients' size, indicated by their height. Moreover, most patients who sustained ACL injuries were males, who tend to participate in more intense sports, such as football and basketball, which carry an increased risk of injury. By screening athletes for these anatomical variations, at-risk individuals could be identified before they sustain an ACL rupture, allowing for early intervention strategies. For elite athletes, where performance and injury avoidance are paramount, this could lead to longer careers, fewer injuries, and optimized performance outcomes.

Differences in anatomy between male and female notch have direct implications for ACL-R surgery and graft choice in clinical settings. Examining the variability in size and shape of the intercondylar notch among individuals might be crucial when planning the ACL reconstruction procedure. During the reconstruction of the ACL, it is important to take into account the anatomical characteristics of each patient in order to potentially restore native ligament function. Thein et al. [33] evaluated the 3D shape and cross-sectional area of the native ACL versus ACL graft and compared the impingement against the intercondylar notch. The presence of a smaller notch size can lead to surgical complications and an elevated risk of ACL re-injury. This statement was confirmed by Park et al. [34] and Wilson et al. [35] who showed that narrow intercondylar notches are associated with greater impingement, which can lead to graft degeneration, and ACL-R failure. Oshima et al. [4] reported that high ratio of graft volume to intercondylar notch volume leads to graft impingement, which results in less graft healing.

The results of our methodology present significant implications for clinical practice in ACL surgery. Knowledge of the notch volume may enhance surgical planning accuracy for several reasons. First, understanding the 3D study of the notch volume enables identification of anatomical landmarks critical for precise femoral tunnel placement. This is particularly relevant in the *trans*-antero-medial technique, where tunnel positioning occurs at over 120° of knee flexion, a point at which visualization of the guide and landmarks becomes challenging. By relying on established landmarks, the surgeon can accurately position the guide at 90° of flexion and maintain it as the knee moves into higher degrees of flexion, improving consistency in tunnel placement.

Second, in the case of ACL revision surgery, identifying the emergence of the previous tunnel within the 3D notch structure, along with analyzing its orientation, helps surgeons determine how to create a new tunnel that minimally interferes with the prior one while maintaining the proper anatomical position.

Third, a preoperative 3D model of the notch provides valuable information about its width, enabling surgeons to anticipate whether a notchplasty is needed and plan accordingly. If the notch is narrow, the surgeon can plan the notchplasty and decide the extent of the volume to be removed.

Future advancements could incorporate this data into robotic surgical systems or augmented reality (AR)-assisted navigation, further increasing precision. However, our approach has limitations. The primary limitation of this study is the absence of longitudinal data to assess the long-term impact of ACL reconstruction surgery. Future research should aim to integrate these analyses into routine preoperative evaluation protocols and explore their potential in customizing ACL reconstruction to the specific anatomical features of each patient.

Etichal approval

This study was performed in line with the principles of the Declaration of Helsinki. Approval was granted by the Ethics Committee of Humanitas Gavazzeni and Castelli (Bergamo, Italy).

CRediT authorship contribution statement

Anna Ghidotti: Writing – review & editing, Writing – original draft, Methodology, Investigation, Data curation, Conceptualization. **Daniele Regazzoni:** Writing – review & editing, Supervision, Funding acquisition, Conceptualization. **Miri Weiss Cohen:** Writing – review & editing, Supervision, Conceptualization. **Caterina Rizzi:** Writing – review & editing, Supervision, Funding acquisition, Conceptualization. **Vincenzo Condello:** Writing – review & editing, Supervision, Funding acquisition, Conceptualization.

Funding

This work was partially supported by Fondazione Humanitas per la Ricerca 5x1000 KCM 023-01.

Declaration of competing interest

The authors declare the following financial interests/personal relationships which may be considered as potential competing interests: The work was partially financially supported by Fondazione Humanitas 5x1000 KCM 023-01.

Acknowledgements

The authors acknowledge the Fondazione Humanitas per la Ricerca for the financial support by grant 5x1000 KCM 023-01.

References

[1] Sanders TL, Maradit Kremers H, Bryan AJ, Larson DR, Dahm DL, Levy BA, et al. Incidence of anterior cruciate ligament tears and reconstruction: A 21-year population-based study. Am J Sports Med 2016;44:1502–7. doi: https://doi.org/10.1177/0363546516629944.

[2] Longo UG, Nagai K, Salvatore G, Cella E, Candela V, Cappelli F, et al. Epidemiology of anterior cruciate ligament reconstruction surgery in Italy: A 15-year nationwide registry study. J Clin Med 2021;10:1–16. doi: https://doi.org/10.3390/JCM10020223.

[3] Zbrojkiewicz D, Scholes C, Zhong E, Holt M, Bell C. Anatomical variability of intercondylar fossa geometry in patients diagnosed with primary anterior cruciate ligament rupture. Clin Anat 2020;33:610–8. doi: https://doi.org/10.1002/CA.23465.

[4] Oshima T, Putnis S, Grasso S, Klasan A, Parker DA. Graft size and orientation within the femoral notch affect graft healing at 1 year after anterior cruciate ligament reconstruction. Am J Sports Med 2020;48:99–108. doi: https://doi.org/10.1177/0363546519885104.

[5] Jha V, Azam MQ, Jain P, Bali SA. Does femoral intercondylar notch volume differ in anterior cruciate ligament-injured adult patients compared to the uninjured? A Meta-Analysis Clin Orthop Surg 2022;14:76. doi: https://doi.org/10.4055/CIOS20163.

[6] Li M, Bai H, Zhang F, Zhou Y, Lin Q, Zhou Q, et al. Automatic segmentation model of intercondylar fossa based on deep learning: a novel and effective assessment method for the notch volume. BMC Musculoskelet Disord 2022;23:426. doi: https://doi.org/10.1186/S12891-022-05378-7.

[7] van Eck CF, Martins CAQ, Lorenz SGF, Fu FH, Smolinski P. Assessment of correlation between knee notch width index and the three-dimensional notch volume. Knee Surg Sports Traumatol Arthrosc 2010;18:1239. doi: https://doi.org/10.1007/S00167-010-1131-3.

[8] Wratten CJE, Tetsworth K, Hohmann E. Three-dimensional femoral notch volume in anterior cruciate ligament-deficient versus anterior cruciate ligament-intact patients: A matched case–control study with inter-gender comparison. Arthroscopy 2015;31:1117–22. doi: https://doi.org/10.1016/J.ARTHRO.2014.12.014.

[9] Zhang C, Zhang X, Fang Z, Wang F, Yuan F, Xie G, et al. The correlation between common 2D femoral notch parameters and 3D notch volume: A retrospective MRI study. BMC Musculoskelet Disord 2019;20:146. doi: https://doi.org/10.1186/S12891-019-2530-3.

[10] Murawski CD, Wolf MR, Araki D, Muller B, Tashman S, Fu FH. Anatomic anterior cruciate ligament reconstruction: current concepts and future perspective. Cartilage 2013;4:27S–37S. doi: https://doi.org/10.1177/1947603513486557.

[11] Quintens L, Herteleer M, Vancleef S, Carette Y, Duflou J, Nijs S, et al. Anatomical variation of the tibia – A principal component analysis. Sci Rep 2019;9:1–10. doi: https://doi.org/10.1038/s41598-019-44092-8.

[12] Pedoia V, Lansdown DA, Zaid M, McCulloch CE, Souza R, Ma CB, et al. Three-dimensional MRI-based statistical shape model and application to a cohort of knees with acute ACL injury. Osteoarthritis Cartilage 2015;23:1695–703. doi: https://doi.org/10.1016/J.JOCA.2015.05.027.

[13] Polamalu SK, Musahl V, Debski RE. Tibiofemoral bony morphology features associated with ACL injury and sex utilizing three-dimensional statistical shape modeling. J Orthop Res 2022;40:87–94. doi: https://doi.org/10.1002/JOR.24952.

[14] Bowes MA, Lohmander LS, Wolstenholme CBH, Vincent GR, Conaghan PG, Frobell RB. Marked and rapid change of bone shape in acutely ACL injured knees – An exploratory analysis of the Kanon trial. Osteoarthritis Cartilage 2019;27:638–45. doi: https://doi.org/10.1016/J.JOCA.2018.12.021.

[15] Ronneberger O, Fischer P, Brox T. U-net: Convolutional networks for biomedical image segmentation. In: Navab N, Hornegger J, Wells W, Frangi A, editors. Medical Image Computing and Computer-Assisted Intervention – MICCAI 2015. MICCAI 2015. Lecture Notes in Computer Science. Cham: Springer; 2015. p. 234–41.

[16] Schlemper J, Oktay O, Schaap M, Heinrich M, Kainz B, Glocker B, et al. Attention gated networks: Learning to leverage salient regions in medical images. Med Image Anal 2019;53:197–207. doi: https://doi.org/10.1016/J.MEDIA.2019.01.012.

[17] Yang D, Xu Z, Li W, Myronenko A, Roth HR, Harmon S, et al. Federated semi-supervised learning for COVID region segmentation in chest CT using multi-national data from China, Italy. Japan Med Image Anal 2021;70:. doi: https://doi.org/10.1016/J.MEDIA.2021.101992101992.

[18] Zhang B, Abbing J, Ghanem A, Fer D, Barker J, Abukhalil R, et al. Towards accurate surgical workflow recognition with convolutional networks and transformers. Comput Methods Biomech Biomed Eng Imaging Vis 2022;10:349–56. doi: https://doi.org/10.1080/21681163.2021.2002191.

[19] Siddique N, Sidike P, Elkin C, Devabhaktuni V. U-Net and its variants for medical image segmentation: Theory and applications. IEEE Access 2021;9:82031–57. doi: https://doi.org/10.1109/ACCESS.2021.3086020.

[20] Wang R, Lei T, Cui R, Zhang B, Meng H, Nandi AK. Medical image segmentation using deep learning: A survey. IET Image Process 2022;16:1243–67. doi: https://doi.org/10.1049/IPR2.12419.

[21] MONAI – Home n.d. Available at: https://monai.io/ [last accessed February 2024].

[22] 3D Slicer image computing platform | 3D Slicer n.d. https://www.slicer.org/ [last accessed February 2024].

[23] Materialise 3-matic | 3D Data Optimization Software n.d. Available at: https://www.materialise.com/en/industrial/software/3-matic?gad_source=1&gclid=EAIaIQobChMI78TKxPbLhAMV5bZoCR3CgAy-EAAYASAAEgLx8vD_BwE [last accessed February 2024].

[24] Hirtler L, Tschematschar K, Kainberger F, Röhrich S. Applicability of semi-quantitative evaluation of the intercondylar notch. Appl Sci 2021;11:5921. doi: https://doi.org/10.3390/APP11135921.

[25] Dauwe J, Vancleef S, De Bondt S, Nijs S. Anatomical variation in humeri: gender and side comparison using statistical shape modelling. Int Orthop 2023;47:1013–20. doi: https://doi.org/10.1007/S00264-023-05713-0/TABLES/2.

[26] Chen C, Ma Y, Geng B, Tan X, Zhang B, Jayswal CK, et al. Intercondylar notch stenosis of knee osteoarthritis and relationship between stenosis and osteoarthritis complicated with anterior cruciate ligament injury. Medicine (Baltimore) 2016;95:. doi: https://doi.org/10.1097/MD.0000000000003439e3439.

[27] Swami VG, Mabee M, Hui C, Jaremko JL. Three-dimensional intercondylar notch volumes in a skeletally immature pediatric population: A magnetic resonance imaging-based anatomic comparison of knees with torn and intact anterior cruciate ligaments. Arthroscopy 2013;29:1954–62. doi: https://doi.org/10.1016/J.ARTHRO.2013.08.031.

[28] Kulseng CPS, Nainamalai V, Grøvik E, Geitung JT, Årøen A, Gjesdal KI. Automatic segmentation of human knee anatomy by a convolutional neural network applying a 3D MRI protocol. BMC Musculoskelet Disord 2023;24:1–12. doi: https://doi.org/10.1186/S12891-023-06153-Y/FIGURES/6.

[29] Almajalid R, Zhang M, Shan J. Fully automatic knee bone detection and segmentation on three-dimensional MRI. Diagnostics (Basel) 2022;12:123. doi: https://doi.org/10.3390/DIAGNOSTICS12010123.

[30] Wang Q, Yao M, Song X, Liu Y, Xing X, Chen Y, et al. Automated segmentation and classification of knee synovitis based on MRI using deep learning. Acad Radiol 2024;31:1518–27. doi: https://doi.org/10.1016/J.ACRA.2023.10.036.

[31] Fayad LM, Rosenthal EH, Morrison WB, Carrino JA. Anterior cruciate ligament volume: Analysis of gender differences. J Magn Reson Imaging 2008;27:218–23. doi: https://doi.org/10.1002/JMRI.21239.

[32] Vrooijink SHA, Wolters F, van Eck CF, Fu FH. Does notch size predict ACL insertion site size? Knee Surg Sports Traumatol Arthrosc 2011;19:S17–21. doi: https://doi.org/10.1007/S00167-011-1503-3.

[33] Thein R, Spitzer E, Doyle J, Khamaisy S, Nawabi DH, Chawla H, et al. The ACL graft has different cross-sectional dimensions compared with the native ACL: Implications for graft impingement. Am J Sports Med 2016;44:2097–105. doi: https://doi.org/10.1177/0363546516645531.

[34] Park SY, Cho JH, Ho JPY, Tu NT, Kim YB, Lee YS. Graft impingement increases anterior cruciate ligament graft signal more than acute graft bending angle: magnetic resonance imaging-based study in outside-in anterior cruciate ligament reconstruction. Knee Surg Sports Traumatol Arthrosc 2023;31:4379–89. doi: https://doi.org/10.1007/S00167-023-07491-Z.

[35] Wilson WT, Hopper GP, O'Boyle M, Henderson L, Blyth MJG. Quantifying graft impingement in anterior cruciate ligament reconstruction. Knee 2022;34:270–8. doi: https://doi.org/10.1016/J.KNEE.2022.01.001.